Metal-insulator transition in the spinel-type Cu1-xNixIr2S4 system

Metal-insulator transition in the spinel-type Cu1-xNixIr2S4 system

Metal-insulator transition in the spinel-type $Cu_{1-x}Ni_xIr_2S_4$ system

Ryo Endoh, Nobuhiro Matsumoto, Susumu Chikazawa, and Shoichi Nagata*
Department of Materials Science and Engineering, Muroran Institute of Technology, 27-1 Mizumoto-cho, Muroran, Hokkaido 050-8585, Japan

Takao Furubayashi and Takehiko Matsumoto
National Research Institute for Metals, 1-2-1 Sengen, Tsukuba, Ibaraki 305-0047, Japan
(Received 8 February 2001; published 25 July 2001)

The normal thiospinel $CuIr_2S_4$ exhibits a temperature-induced metal-insulator (M-I) transition around 230 K with structural transformation, showing hysteresis on heating and cooling. The symmetry changes from a high-temperature cubic phase in a metallic state to low-temperature tetragonal phase in an insulating state. A significant characteristic feature is the absence of localized magnetic moment below T_{M-I}. On the other hand, $NiIr_2S_4$ remains metallic down to 4.2 K without the structural transformation. We have systematically studied the structural transformation and electrical and magnetic properties of $Cu_{1-x}Ni_xIr_2S_4$. The variation of the metal-insulator transition with Ni concentration x is presented. A phase diagram between T_{M-I} and x will be provided for the $Cu_{1-x}Ni_xIr_2S_4$ system. The T_{M-I} varies drastically from 226 to 88 K with x from 0.00 to 0.13 and disappears around $x=0.15$. For $0.08 \leqslant x \leqslant 0.13$, the cubic and tetragonal phases coexist below T_{M-I}. For a high-temperature metallic phase, the value of the Pauli paramagnetic susceptibility increases monotonically with x, which shows $dD(\varepsilon)/d\varepsilon<0$ at the Fermi energy ε_F, through the decrease of the free-electron number density, where $D(\varepsilon)$ is the electronic density-of-state on the basis of a nearly free-electron model. By the introduction of a Ni ion to the A-site of $CuIr_2S_4$ in the spinel structure, whether the localized magnetic moment below T_{M-I} arises or not will be discussed.

DOI: 10.1103/PhysRevB.64.075106 PACS number(s): 71.30.+h, 75.50.−y, 61.10.−i, 72.80.Ga

I. INTRODUCTION

Chalcogenide copper thiospinels have a large variety of physical properties. In particular, much of research for the metal-insulator transition in $CuIr_2S_4$ has been extensively done in the last decade.[1–21] Sulfides $CuIr_2S_4$ and $NiIr_2S_4$ have a cubic normal spinel structure. Cu and Ni ions occupy the A (tetrahedral) sites and Ir ions occupy the B (octahedral) sites. $CuIr_2S_4$ exhibits a temperature-induced metal-insulator (M-I) transition around 230 K with structural transformation, showing hysteresis on heating and cooling. With decreasing temperature, a symmetry changes from cubic to tetragonal symmetry, accompanying an alteration from the Pauli paramagnetism in high-temperature metallic state to diamagnetism due to the atomic core orbital in the insulating state. Detailed structural analysis of the low-temperature phase has been done by Ishibashi *et al.*[22,23] The majority of electrical carriers in the semiconductive (insulating) phase is holes, which is confirmed by Hall-effect measurements.[24,25] The photoemission[26] and Cu nuclear-magnetic-resonance (NMR) measurements[27] have verified that Cu ion has a monovalent state of Cu^+ in the low-temperature insulating state. On the basis of the simple ionic picture, therefore, the driving force of cooperative Jahn-Teller distortion by Cu^{2+} ions disappears. Consequently, the Jahn-Teller distortion effect based on the ionic picture, is not the main cause for the structural transformation in $CuIr_2S_4$, however, we do not exclude a band Jahn-Teller effect, which gives rise to the M-I transition.[4] Many Cu-NMR measurements have been made.[28–33]

On the other hand, $NiIr_2S_4$ does not indicate any M-I transition, nor the structural transformation. $NiIr_2S_4$ remains metallic down to 4.2 K without anomalous behavior. It is an important subject to investigate the variation of physical properties for the M-I transition by substitution of Ni for Cu. We expect that the gradual changes of M-I transition can be observed by this chemical modification with a variation of the number of d electrons. The clarification of the origin and mechanism of the M-I transition may germinate from these variations. Furthermore, the superconducting state has recently been discovered for the new system of $Cu_{1-x}Zn_xIr_2S_4$.[34,35] This Zn-substitution system is the first example for the A-site substitution.

The present investigation of a Ni-substitution system is the second example for the A-site substitution. From the viewpoint of comparison between the number of d electrons in $CuIr_2S_4$, this Ni system is deficient, on the contrary, the Zn system is excessive in d electron number. We have successfully synthesized the specimens of $Cu_{1-x}Ni_xIr_2S_4$ and carried out a systematic experimental study of structural, electrical, and magnetic properties of $Cu_{1-x}Ni_xIr_2S_4$. The increase of Ni concentration x leads to a remarkable change in the magnetic and electrical features. In particular, the characteristic variation has been observed in the magnetic behavior for the Cu-rich concentration region $0.05<x<0.15$. A phase diagram between temperature T and Ni concentration x has been provided experimentally for the system of $Cu_{1-x}Ni_xIr_2S_4$. Other substituted systems have been extensively investigated.[36–41]

II. EXPERIMENTAL METHODS

The polycrystalline specimens were prepared by a direct solid-state reaction. Mixtures of high-purity fine powders of

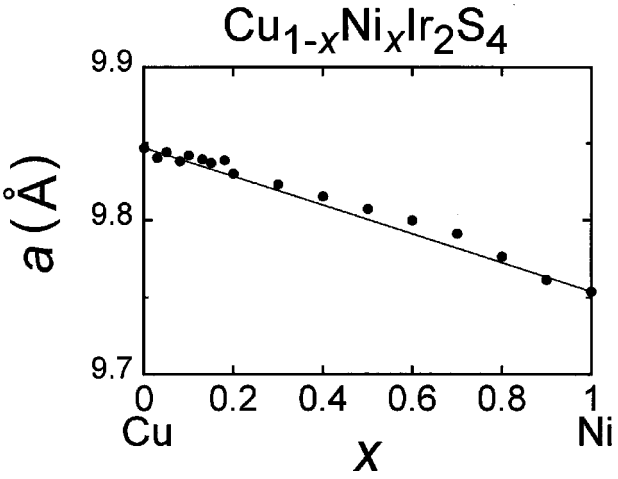

FIG. 1. The lattice constant a as a function of Ni concentration x at room temperature.

Cu (purity 99.99 %), Ni (99.99 %), Ir (99.99 %), and S (99.999 %) with nominal stoichiometry, were heated in sealed quartz tubes to 1123 K and kept at this temperature for 10 days. The resultant powder specimens were reground and pressed to rectangular bars and then were heated to 1123 K for 2 days. Since it was harder to prepare the high-purity specimens for higher Ni concentration $x>0.40$, they were obtained by repeating this process several times. A pure $NiIr_2S_4$ sample was obtained by heating to 1423 K for 3 days. The identification of the crystal structure and the determination of the lattice constants were carried out by the powder x-ray diffraction method using Cu $K\alpha$ radiation from room temperature to 10 K. Low-temperature x-ray experiments down to 10 K were attained by a closed-cycle helium refrigerator.

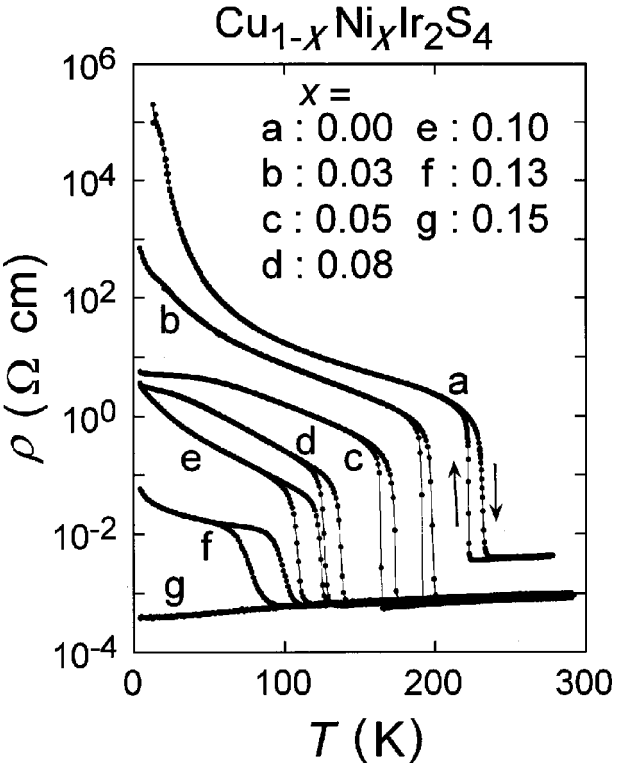

FIG. 2. Temperature dependence of electrical resistivity ρ for sintered specimens $Cu_{1-x}Ni_xIr_2S_4$ for $0.00\leqslant x\leqslant 0.15$.

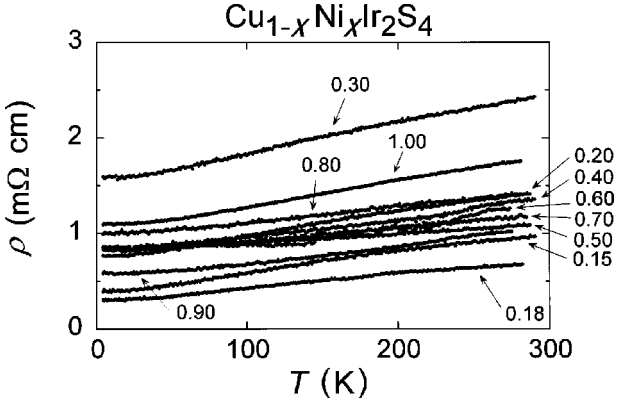

FIG. 3. Temperature dependence of electrical resistivity ρ for sintered specimens $Cu_{1-x}Ni_xIr_2S_4$ for $0.15\leqslant x\leqslant 1.00$.

The resistivity ρ of sintered specimens with dimensions of about $2\times2\times10$ mm^3 was measured by a standard dc four-probe method over a temperature range of 4.2 K to room temperature. Silver paste was used to fabricate electrodes. The dc magnetic susceptibility χ of powder specimens was measured with a quantum design rf superconducting quantum interference device magnetometer over a range

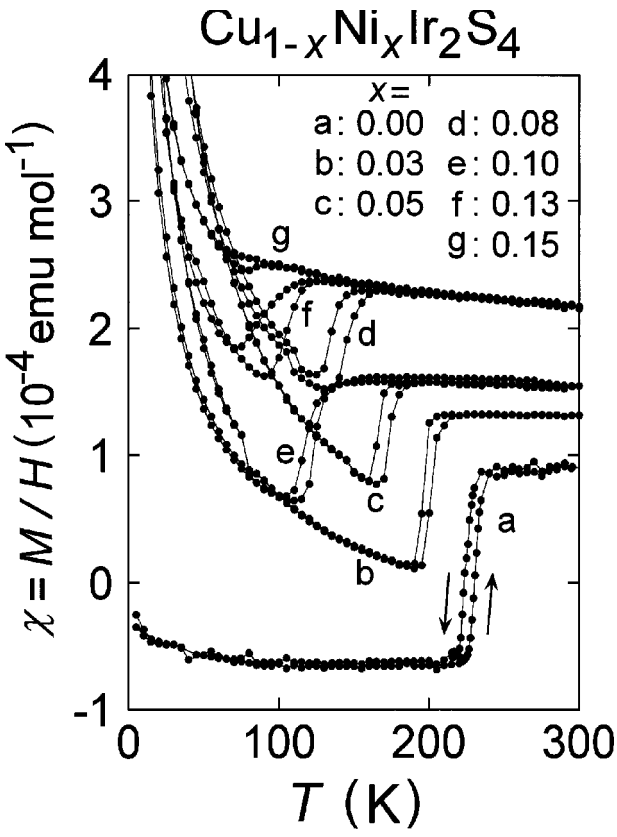

FIG. 4. Magnetic susceptibility vs temperature of $Cu_{1-x}Ni_xIr_2S_4$ for $0.00\leqslant x\leqslant 0.15$. The applied magnetic field is 10.000 kOe.

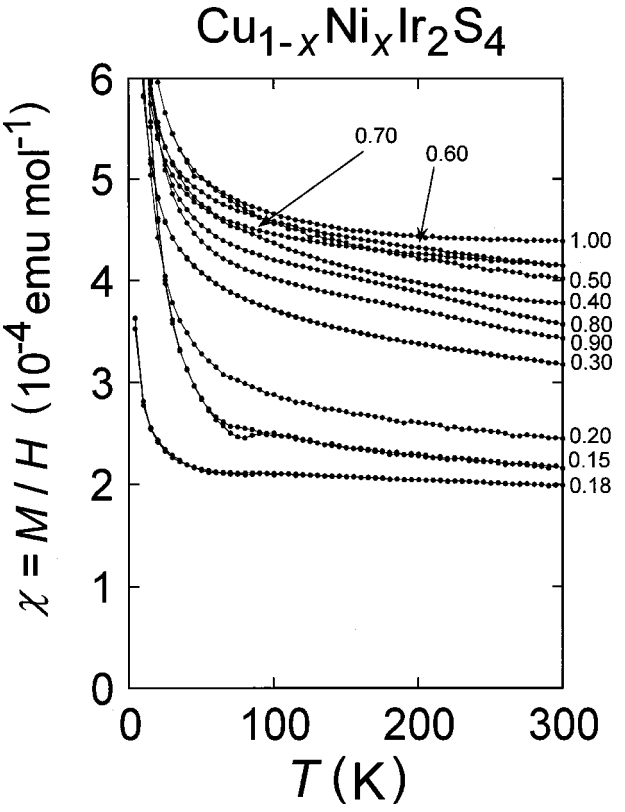

FIG. 5. Magnetic susceptibility vs temperature of $Cu_{1-x}Ni_xIr_2S_4$ for $0.15 \leqslant x \leqslant 1.00$. The applied magnetic field is 10.000 kOe.

of $4.2 \leqslant T \leqslant 300$ K at intervals of 5 K in an applied magnetic field of 10 kOe.

III. RESULTS AND DISCUSSION

A. Variation of metal-insulator transition in $Cu_{1-x}Ni_xIr_2S_4$

Powder x-ray diffraction patterns at room temperature confirm that $Cu_{1-x}Ni_xIr_2S_4$ has the normal spinel-type structure in all the Ni-concentration range, although a small amount of impurities was found in a rather higher Ni-concentration region. The value of lattice constant a varies from 9.847 Å for $x=0.00$ to 9.754 Å and for $x=1.00$ at room temperature, as shown in Fig. 1.

Figures 2 and 3 show the temperature dependence of electrical resistivity for the sintered specimens in the Cu-rich region ($0.00 \leqslant x \leqslant 0.15$) and the higher x region of $0.15 \leqslant x$. The resistivity of $CuIr_2S_4$, drops abruptly by nearly three orders of magnitude around 230 K with temperature hysteresis. With increasing Ni concentration x, the M-I transition temperature $T_{M\text{-}I}$ decreases steeply and the height of the jump at $T_{M\text{-}I}$ becomes smaller. The temperature dependence of the resistivity below $T_{M\text{-}I}$ changes gradually from the semiconductive behavior to metallic one. Above $x=0.15$, simple metallic behavior is observed without the sharp jump in the resistivity, as can be seen in Fig. 3. It is hard to judge the concentration dependence of the absolute magnitude of the resistivity because of the somewhat experimental uncertainty due to the filling density of the sintered specimens.

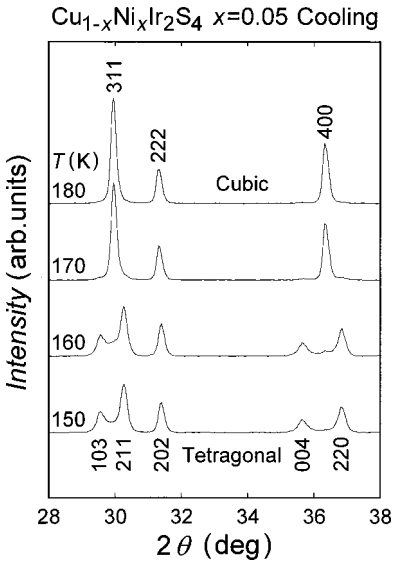

FIG. 6. Temperature dependence of the powder x-ray diffraction pattern for $x=0.05$ upon cooling. At 150 K, the only tetragonal phase is detected.

Figures 4 and 5 show the temperature dependence of magnetic susceptibility for the powder specimens in the two Ni-concentration regions of $0.00 \leqslant x \leqslant 0.15$, and the higher x region of $0.15 \leqslant x \leqslant 1.00$. The value of χ is obtained by dividing the magnetization M by the applied magnetic field H. Measurements were carried out on warming and cooling at a constant applied magnetic field of 10 kOe. The $T_{M\text{-}I}$ in the resistivity corresponds exactly to the steplike anomaly of the susceptibility. With increasing Ni concentration x, the temperature dependence of the susceptibility becomes steeper below $T_{M\text{-}I}$ as seen in Fig. 4. For $x \leqslant 0.18$, the temperature dependence of the susceptibility indicates no steplike

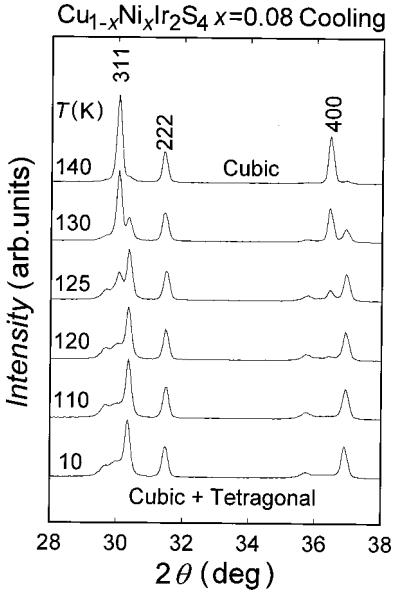

FIG. 7. Temperature dependence of the powder x-ray diffraction pattern for $x=0.08$ upon cooling. It is noted that the coexistence of the tetragonal and cubic phases is detected even at 10 K.

TABLE I. Mol fraction of tetragonal phase in the low-temperature crystal structure for $x \leqslant 0.13$. Between $x = 0.08$ and 0.13, the coexistence of the tetragonal and cubic phases is observed on the basis of the x-ray Rietveld analysis.

x	Mol fraction of tetragonal phase (%)	Crystal structure
0.03	100	Tetragonal
0.05	100	
0.08	75–85	Cubic
0.10	55–65	plus
0.13	35–45	Tetragonal

anomaly. It should be noticed that the magnetic susceptibility of $CuIr_2S_4$, in the low-temperature insulating phase, indicates nonmagnetism except the small amount of the diamagnetism. The diamagnetic susceptibility is due to atomic cores and is estimated to be an order of 10^{-4} emu mol^{-1} for $Cu_{1-x}Ni_xIr_2S_4$ by using the Pascal additive law[42] and this order of magnitude is reasonable.

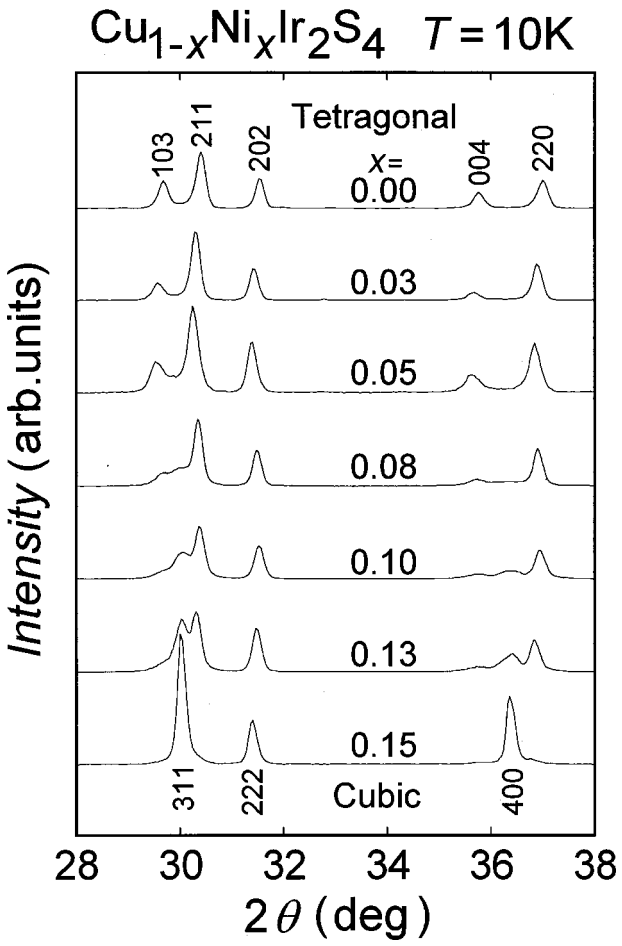

FIG. 8. X-ray diffraction pattern for $0.00 \leqslant x \leqslant 0.15$ at 10 K over the angle range of $28 \leqslant 2\theta \leqslant 38°$.

B. Structural transformation

Figure 6 shows the powder x-ray diffraction patterns of the sample $x = 0.05$ at various temperatures near $T_{M\text{-}I}$. The structural transformation is observed from cubic to tetragonal symmetry with decreasing temperature. At 190 K, the diffraction peaks can be indexed on the cubic symmetry with the space group $Fd\bar{3}m$. Between 170 and 180 K, the coexistence of the cubic and tetragonal symmetry can be manifestly seen, where two peaks from the cubic and three from the tetragonal symmetry are overlapped in the region of diffraction angle $29 \leqslant 2\theta \leqslant 32°$. One peak arises from the cubic and two peaks from the tetragonal overlap in $35 \leqslant 2\theta \leqslant 37°$. The diffraction peaks at 160 K are indexed on the tetragonal symmetry with the space group $I4_1/amd$. The temperature of structural transformation corresponds fairly well to the midpoint of the abrupt increase in the resistivity, which also coincides with that of the susceptibility.

Between $0.08 \leqslant x \leqslant 0.13$, the temperature region in the coexistence of the cubic and tetragonal phases spreads to the lowest temperature of 10 K in our measurements as shown in Fig. 7. The mol rate of mixing of the tetra and cubic phases is evaluated in Table I by using the two phases Rietveld analysis program (RIETAN).[43] The intensity of the tetragonal phase decreases with increasing x, as shown in Table I, which includes appreciable errors because of the overlapping for the x-ray peaks. Figure 8 shows the concentration dependence of diffraction patterns over a range of $0.00 \leqslant x \leqslant 0.15$ at the constant temperature of 10 K. Specimens of $x = 0.00$, 0.03, and 0.05 have almost tetragonal structure at 10 K. In the concentration range of $0.08 \leqslant x \leqslant 0.13$, there exist both tetragonal and cubic phases. The specimen for $x \leqslant 0.15$ has only cubic phase. We speculate that this coexistence occurs not in the macroscopic but in a rather microscopic scale and that the phases mix homogeneously, each providing a percolation system. This conjecture is indirectly supported by the macroscopic results that the temperature dependence of the resistivity and magnetic susceptibility vary not irregularly but fairly smoothly over a wide concentration region.

The M-I transition temperature $T_{M\text{-}I}$ of $CuIr_2S_4$ increases under high pressure,[2,5] which is unusual. The insulating phase of $CuIr_2S_4$ is stabilized under pressure. This is contrary to the effect of pressure in most oxides that exhibit M-I

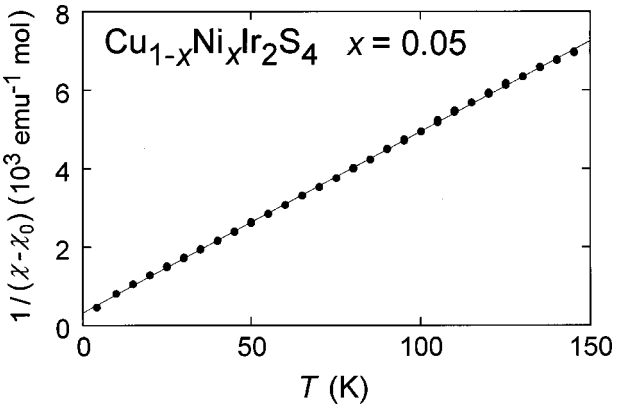

FIG. 9. Temperature dependence of the inverse susceptibility $(\chi - \chi_0)^{-1} = (M/H)^{-1}$ for $x = 0.05$.

TABLE II. Summary of the magnetic properties of $Cu_{1-x}Ni_xIr_2S_4$ for $x \leqslant 0.13$: (a) The value of effective magnetic moment of the Ni ion, where it is assumed that all the Ni ions possess a localized moment. (b) The value of the magnetic moment of the Ni ion, assuming that the Ni ion in only the tetragonal phase possesses the localized moment and the Ni ion in the cubic phase does not have the localized moment.

	Curie-Weiss law ($T < T_{M\text{-}I}$)					
x	χ_0 (emu / mol f.u.)	C (emu K/ mol f.u.)	θ (K)	(a)μ_{eff}/Ni ion (for all the Ni ion)	(b)μ_{eff}/Ni ion (for the Ni ion in only the tetragonal phase)	Crystal structure
0.00						
0.03	-0.564×10^{-4}	1.330×10^{-2}	-5.87	1.88	1.88	Tetragonal
0.05	-0.474×10^{-4}	2.165×10^{-2}	-7.09	1.86	1.86	
0.08	0.326×10^{-4}	1.680×10^{-2}	-6.20	1.30	1.41–1.50	Cubic
0.10	-0.076×10^{-4}	0.7839×10^{-2}	-3.90	0.792	0.98–1.07	plus
0.13	0.661×10^{-4}	0.8895×10^{-2}	-5.61	0.740	1.10–1.25	Tetragonal

transition, including V_2O_3[44] and Fe_3O_4.[45,46] In the Mott picture of the *M-I* transition, high pressure should increase the electron orbital overlap, thus stabilizing the metallic state.

The Se substitution for sulfur, $CuIr_2(S_{1-x}Se_x)_4$, expands the lattice and reduces the chemical pressure, which could decrease $T_{M\text{-}I}$, as observed.[12] On the other hand, *B*-site cation substitution systems of $Cu(Ir_{1-x}Ti_x)_2S_4$,[47] $Cu(Ir_{1-x}Cr_x)_2S_4$,[14] $Cu(Ir_{1-x}Rh_x)_2S_4$,[15] and $Cu(Ir_{1-x}Pt_x)_2S_4$[16] exhibit the decrease of $T_{M\text{-}I}$ by substitution. Furthermore, the *A*-site cation substitution system of $Cu_{1-x}Zn_xIr_2S_4$,[34] also shows the decrease of $T_{M\text{-}I}$, as observed of $Cu_{1-x}Ni_xIr_2S_4$ in the present paper. In all the cases of cation and anion substitution, the characteristics of the decrease of $T_{M\text{-}I}$ with the value of x is the fairly same manner as in the present paper. A common feature is that the coexistence of cubic and tetragonal phases appear in the temperature region around $T_{M\text{-}I}$ and this intermediate region expands progressively with the value of x. Simple comparison between the ionic volume for the substituted element and the strength of chemical pressure (or the result of high pressure measurements of $CuIr_2S_4$) is unreasonable, whereas the local distortion and symmetry change by substitution is more significant. Considerable emphasis was placed on the short-range and local configuration.[15]

The global experimental aspects of these substituted systems for $CuIr_2S_4$ resemble fairly the general features of ''martensitic transformation,'' which occurs in steels, some alloys, and also inorganic compounds without atom diffusion. We adopt the concept of martensitic transformation for the $CuIr_2S_4$ system. Hear, we point out one important result of the hydrostatic pressure experiment for Cu–Al–Ni and Ti–Ni alloys, which are well known as the martensitic transformation. The transformation temperature of these alloys increases linearly with increasing pressure,[48] as observed in $CuIr_2S_4$.[2,5] The difference in volume, which is $V^m - V^p$, where V^m and V^p are the volumes of martensite and parent phases, respectively; $V^m - V^p$ is negative (-0.3%) for the Cu–Al–Ni alloy.[48] In the present compound $CuIr_2S_4$, the martensite and parent phases correspond to the tetragonal and cubic phases. The volume contraction of $CuIr_2S_4$ at the structure transformation from cubic to tetragonal is 0.7%, i.e., $V^m - V^p$ is negative (-0.7%).[2] It should be noticed that the direct comparison of pressure effect between $CuIr_2S_4$ and the Invar alloy, which exhibits the martensitic transformation, is irrelevant because of the influence of a spontaneous volume magnetostriction. We hope that analysis and discussion on mechanical driving force, chemical driving force, and/or electronic structure that induce the crystal transformation, will be made fruitful from the viewpoint of the ''martensitic transformation.''[48]

C. Relationship between the value of the effective magnetic moment and the structural transformation

The x-ray Rietveld analysis at 10 K shows the mol fraction of the tetragonal phase in Table I, where the about 40% of the specimen exists as the tetragonal phase for $x = 0.13$. It is postulated that the low-temperature tetragonal phase has

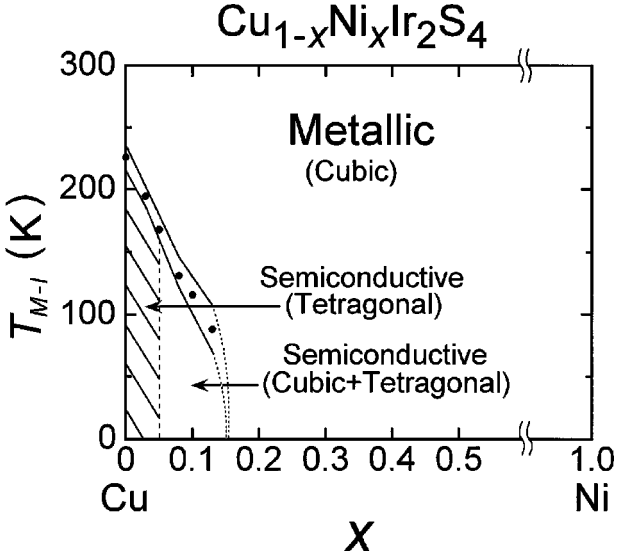

FIG. 10. A phase diagram of $Cu_{1-x}Ni_xIr_2S_4$ for temperature vs concentration x. The solid circles indicate the *M-I* transition temperature $T_{M\text{-}I}$. Two solid curves show the width of the temperature hysteresis for the *M-I* transition, which corresponds fairly well to the structural transformation; see the text.

the insulating property and the low-temperature cubic phase remains basically metallic, therefore, the localized magnetic moment arises from the tetragonal phase only. Furthermore, we assume that only the tetragonal phase Ni ion possesses a localized magnetic moment. The magnetic susceptibility is analyzed on the basis of the modified Curie-Weiss law, $\chi = \chi_0 + C/(T-\theta)$, where χ_0 is the temperature-independent susceptibility, C is the Curie constant, and θ is the Weiss temperature. Figure 9 indicates an example of the result for $x=0.05$. Table I shows the summary of the experimental results of the magnetic properties below $T_{M\text{-}I}$. It is hard to draw a definite conclusion for the induced magnetic moment that originates from the Ni substitution. Nevertheless, we can interpret the Curie-type signal by an effective magnetic moment per Ni ion in the low-temperature tetragonal phase to be $s=1/2$ at best, having $2\sqrt{s(s+1)}=1.73$. The physical meaning for this value is still uncertain at present.

The high-temperature cubic metallic phase shows Pauli paramagnetism, i.e., basically no temperature dependence of $\chi(T)$ for all specimens. The susceptibility at 300 K in the metallic state increases monotonically with the Ni concentration x, as can be seen in Figs. 4 and 5, where this tendency continues up to $x=0.70$, which is close to the limiting value observed in the high purity of specimens. This experimental result shows a trend opposite to that observed in the $Cu_{1-x}Zn_xIr_2S_4$ system; see Ref. 34. The Zn substitution leads to decreasing the magnitude of the susceptibility for the high-temperature cubic phase. This characteristic difference for the variation of the Pauli paramagnetism stands for the derivative of the density-of-state $D(\varepsilon)$ near the Fermi surface with respect to negative electronic energy, $dD(\varepsilon)/d\varepsilon < 0$, on the basis of rigid-band model for a nearly free electron. We suggest that the hole occupation in the density-of-states of $CuIr_2S_4$ goes up or down with Ni or Zn substitution for Cu, respectively.

For $x<0.15$, the minimum value of the susceptibility at just below the $T_{M\text{-}I}$ goes up systematically with increasing x. This result reflects two factors, first the fraction of low-temperature cubic phase increases with x, and second the density-of-state in the metallic state increases with x owing to the substitution of Ni, which is mentioned above.

In Fig. 5, the rapid increase in the susceptibility at low temperatures may be due to the existence of the localized spins at an impurity site or at other kinds of lattice imperfection. The experimental estimation for effective magnetic moment per Ni ion from the Curie-like behavior, gives the values to be 0.631, 0.637, 0.589, 0.495, and 0.286 for $x=0.20$, 0.30, 0.40, 0.50, and 0.70, respectively. There is no indication of any systematic variation of the effective moment with the value of x. Then, there seems to be no intrinsic localized magnetic moment in high-temperature cubic phase. Kang *et al.* has presented electron paramagnetic resonance spectra and the suggestion about the structural defect associated with the rapid increase in the susceptibility at low temperature,[49–51] which is in agreement with our explanation. The structure imperfection might come from the sulfur nonstoichiometry. The influence of the sulfur nonstoichiometry on the *M-I* transition in $CuIr_2S_{4+y}$ was investigated by Somasundaram *et al.*[38] The formal valence of Cu or Ir should change as one varies the sulfur composition. Summarizing the magnetic properties in Table II, it should be noted that the numerical value of the effective magnetic moment in the low-temperature phase includes an error from the unknown quantity of the structural defects that carry a magnetic moment.

D. Phase diagram of $Cu_{1-x}Ni_xIr_2S_4$

Figure 10 shows a phase diagram for T vs x, which simplifies the rather complicated structural and electrical characteristics in the system $Cu_{1-x}Ni_xIr_2S_4$. Solid circles for $x<0.15$ show the abrupt *M-I* transition temperature $T_{M\text{-}I}$ in the resistivity and the susceptibility. This $T_{M\text{-}I}$ decreases linearly with x. For $x=0.15$, the temperature dependence of the resistivity varies with simple metallic behavior. The *M-I* transition is seen in the region of $0.00 \leqslant x < 0.15$. The cubic phase at high temperatures changes to the tetragonal one at low temperatures as indicated by the shaded area. For $0.05 < x < 0.15$, the coexistence of cubic and tetragonal phases has been observed below $T_{M\text{-}I}$.

ACKNOWLEDGMENTS

The authors would like to thank Mr. M. Hayashi for his help in the experiments. The present research was supported financially by a Grant-in-Aid for Scientific Research (No. 11640329 and No. 12046204) from the Ministry of Education, Science, Sports, and Culture of Japan. Support from The Japan Securities Scholarship Foundation is also gratefully acknowledged.

*Author to whom correspondence should be addressed; Electronic address: naga-sho@mmm.muroran-it.ac.jp

[1] S. Nagata, T. Hagino, Y. Seki, and T. Bitoh, Physica B **194-196**, 1077 (1994).

[2] T. Furubayashi, T. Matsumoto, T. Hagino, and S. Nagata, J. Phys. Soc. Jpn. **63**, 3333 (1994).

[3] T. Hagino, Y. Seki, and S. Nagata, Physica C **235-240**, 1303 (1994).

[4] T. Hagino, T. Tojo, T. Atake, and S. Nagata, Philos. Mag. B **71**, 881 (1995).

[5] G. Oomi, T. Kagayama, I. Yoshida, T. Hagino, and S. Nagata, J. Magn. Magn. Mater. **140-144**, 157 (1995).

[6] K. Balcerek, Cz. Marucha, R. Wawryk, T. Tyc, N. Matsumoto, and S. Nagata, in *11th Seminar on Phase Transitions and Critical Phenomena, Wroclaw and Polanica Zdrój, Poland, May, 1998*, Series in Physics and Chemistry of Solids, edited by M. Kazimierski (Institute of Low Temperature and Structure Research, Polish Academy of Sciences, Wroclaw, 1998), p. 110.

[7] K. Balcerek, Cz. Marucha, R. Wawryk, T. Tyc, N. Matsumoto, and S. Nagata, Philos. Mag. B **79**, 1021 (1999).

[8] T. Oda, M. Shirai, N. Suzuki, and K. Motizuki, J. Phys.: Condens. Matter **7**, 4433 (1995).

[9] E.Z. Kurmaev *et al.*, Solid State Commun. **108**, 235 (1998).

[10] A.T. Burkov, T. Nakama, K. Shintani, K. Yagasaki, N. Matsu-

moto, and S. Nagata, Phys. Rev. B **61**, 10 049 (2000).
[11] A.T. Burkov, T. Nakama, K. Shintani, K. Yagasaki, N. Matsumoto, and S. Nagata, Physica B **281-282**, 629 (2000).
[12] S. Nagata, N. Matsumoto, Y. Kato, T. Furubayashi, T. Matsumoto, J.P. Sanchez, and P. Vulliet, Phys. Rev. B **58**, 6844 (1998).
[13] N. Matsumoto and S. Nagata, J. Cryst. Growth **210**, 772 (2000).
[14] R. Endoh, N. Matsumoto, J. Awaka, and S. Nagata, J. Phys. Chem. Solids (to be published).
[15] N. Matsumoto, R. Endoh, S. Nagata, T. Furubayashi, and T. Matsumoto, Phys. Rev. B **60**, 5258 (1999).
[16] N. Matsumoto, Y. Yamauchi, H. Takano, and S. Nagata, Int. J. Inorg. Mater. (to be published).
[17] M. Hayashi, M. Nakayama, T. Nanba, T. Matsumoto, J. Tang, and S. Nagata, Physica B **281-282**, 631 (2000).
[18] J. Tang, T. Matsumoto, T. Naka, T. Furubayashi, S. Nagata, and N. Matsumoto, Physica B **259-261**, 857 (1999).
[19] J. Tang, T. Matsumoto, T. Furubayashi, T. Kosaka, S. Nagata, and Y. Kato, J. Magn. Magn. Mater. **177-181**, 1363 (1998).
[20] T. Furubayashi, T. Kosaka, J. Tang, T. Matsumoto, Y. Kato, and S. Nagata, J. Phys. Soc. Jpn. **66**, 1563 (1997).
[21] J. Tang, T. Furubayashi, T. Kosaka, S. Nagata, Y. Kato, H. Asano, and T. Matsumoto, Rev. High Pressure Sci. Technol. **7**, 496 (1998).
[22] R. Oshima, H. Ishibashi, K. Tanioka, and K. Nakahigashi, in *Proceedings the International Conference On Solid-Solid Phase Transformations '99 (JIMIC-3)*, edited by M. Koiwa, K. Otsuka, and T. Miyazaki (The Japan Institute of Metals, 1999), p. 895.
[23] H. Ishibashi, T. Sakai, and K. Nakahigashi, J. Magn. Magn. Mater. (to be published).
[24] J. Tang, S. Uji, T. Terakura, T. Naka, T. Matsumoto, T. Furubayashi, A. Matsushita, S. Nagata, and N. Matsumoto, Abstracts of the Meeting of the Physical Society of Japan, (53rd Annual Meeting, Funabashi, March–April 1998), Part. 3, p. 632, 2p-R-9 (in Japanese).
[25] H. Kang, K. Bärner, I.V. Medvedeva, P. Mandal, A. Poddar, and E. Gmelin, J. Alloys Compd. **267**, 1 (1998).
[26] J. Matsuno, T. Mizokawa, A. Fujimori, D.A. Zatsepin, V.R. Galakhov, E.Z. Kurmaev, Y. Kato, and S. Nagata, Phys. Rev. B **55**, R15 979 (1997).
[27] K. Kumagai, S. Tsuji, T. Hagino, and S. Nagata, in *Spectroscopy of Mott Insulators and Correlated Metals*, Springer Series in Solid-State Sciences, Vol. 119, edited by A. Fujimori and Y. Tokura (Springer-Verlag, Berlin, 1995), p. 255.
[28] S. Tsuji, K. Kumagai, N. Matsumoto, Y. Kato, and S. Nagata, Physica B **237-238**, 156 (1997).
[29] S. Tsuji, K. Kumagai, N. Matsumoto, and S. Nagata, Physica C **282-287**, 1107 (1997).
[30] K. Kumagai, K. Kakuyanagi, R. Endoh, and S. Nagata, Physica C **341-348**, 741 (2000).
[31] Y. Kishimoto, T. Ohno, S. Nagata, N. Matsumoto, T. Kanashiro, Y. Michihiro, and K. Nakamura, Physica C **281-282**, 634 (2000).
[32] A. Goto, T. Shimizu, G. Cao, H. Suzuki, H. Kitazawa, and T. Matsumoto, Physica C **341-348**, 737 (2000).
[33] A. Goto, T. Shimizu, G. Cao, H. Suzuki, H. Kitazawa, and T. Matsumoto, J. Phys. Soc. Jpn. **70**, 9 (2001).
[34] H. Suzuki, T. Furubayashi, G. Cao, H. Kitazawa, A. Kamimura, K. Hirata, and T. Matsumoto, J. Phys. Soc. Jpn. **68**, 2495 (1999).
[35] G. Cao, H. Suzuki, T. Furubayashi, H. Kitazawa, and T. Matsumoto, Physica B **281-282**, 636 (2000).
[36] P. Somasundaram, J.M. Honig, T.M. Pekarek, and B.C. Crooker, J. Appl. Phys. **79**, 5401 (1996).
[37] F.A. Chudnovskii, A.L. Pergament, G.B. Stefanovich, P. Somasundaram, and J.M. Honig, Phys. Status Solidi A **162**, 601 (1997).
[38] P. Somasundaram, D. Kim, J.M. Honig, and T.M. Pekarek, J. Appl. Phys. **81**, 4618 (1997).
[39] P. Somasundaram, D. Kim, J.M. Honig, T.M. Pekarek, T. Gu, and A.I. Goldman, J. Appl. Phys. **83**, 7243 (1998).
[40] S. Nagata, S. Yasuzuka, Y. Kato, T. Hagino, M. Matsumoto, N. Kijima, and S. Ebisu, Czech. J. Phys. **46** S5, 2425 (1996).
[41] G.L.W. Hart, W.E. Pickett, E.Z. Kurmaev, D. Hartmann, M. Neumann, A. Moewes, D.L. Ederer, R. Endoh, K. Taniguchi, and S. Nagata, Phys. Rev. B **61**, 4230 (2000).
[42] E. Konig and G. Konig, in *Magnetic Properties of Coordination and Organometallic Transition Metal Compounds*, edited by K.-H. Hellwege and A. M. Hellwege, Landolt-Börnstein, New Series, Group II, Vol. 8 (Springer-Verlag, Berlin, 1976), p.27.
[43] F. Izumi, in *The Rietveld Method*, edited by R.A. Young (Oxford University, Oxford, 1993), Chap. 13.
[44] D.B. McWhan, A. Menth, J.P. Remeika, W.F. Brinkman, and T.M. Rice, Phys. Rev. B **7**, 1920 (1973).
[45] G.Kh. Rozenberg, G.R. Hearne, M.P. Pasternak, P.A. Metcalf, and J.M. Honig, Phys. Rev. B **53**, 6482 (1996).
[46] S. Todo, N. Takeshita, T. Kanehara. T. Mori, and N. Môri, J. Appl. Phys. (to be published).
[47] S. Nagata and S. Ito (unpublished).
[48] T. Kakeshita, T. Saburi, and K. Shimizu, *Proceedings the International Conference on Martensitic Transformation '98 (ICOMAT-98)*, edited by M. Ahlers, G. Kostorz, and M. Sade (Elsevier, Amsterdam, 1999); Mater. Sci. Eng., A **273-275**, 21 (1999).
[49] H. Kang, K. Bärner, H. Rager, U. Sondermann, P. Mandal, I.V. Medvedeva, and E. Gmelin, J. Alloys Compd. **306**, 6 (2000).
[50] H. Kang, P. Mandal, I.V. Medvedeva, K. Bärner, A. Poddar, and E. Gmelin, Phys. Status Solidi A **163**, 465 (1997).
[51] H. Kang, P. Mandal, I.V. Medvedeva, J. Liebe, G.H. Rao, K. Bärner, A. Poddar, and E. Gmelin, J. Appl. Phys. **83**, 6977 (1998).